Fiber strain sensor based on a pi-phase-shifted Bragg grating and the Pound-Drever-Hall technique

Fiber strain sensor based on a π-phase-shifted Bragg grating and the Pound-Drever-Hall technique

D. Gatti,[1] **G. Galzerano,**[1*] **D. Janner,**[2]
S. Longhi[1]**, and P. Laporta**[1]

[1]*Istituto di Fotonica e Nanotecnologie - Consiglio Nazionale delle Ricerche and Dipartimento di Fisica del Politecnico di Milano, 20133 Milano, Italy*
[2]*ICFO - Institut de Ciencies Fotoniques, Mediterranean Technology Parc, 08860 Castelldefels (Barcelona), Spain*
[*]*Corresponding author: gianluca.galzerano@fisi.polimi.it*

Abstract: A fiber strain sensor based on a π-phase-shifted Bragg grating and an extended cavity diode laser is proposed. Locking the laser frequency to grating resonance by the Pound-Drever-Hall technique results in a strain power spectral density $S_\varepsilon(f) = (3\times10^{-19} f^{-1} + 2.6\times10^{-23})\ \varepsilon^2$/Hz in the Fourier frequency range from 1 kHz to 10 MHz (ε being the applied strain), corresponding to a minimum sensitivity of 5 pεHz$^{-1/2}$ for frequencies larger than 100 kHz.

OCIS codes: (060.3735) Fiber Bragg gratings; (060.2370) Fiber optics sensors; (120.5050) Phase measurement; (140.3425) Laser stabilization; (120.0280) Remote sensing and sensor.

References and links

1. A. Othenos and K. Kalli, *Fiber Bragg grating: Fundamental and applications in telecommunications and sensing.* Norwood: Artech House, 1999.
2. Y. J. Rao and S. Huang, "Applications of fiber optic sensors," in *Fiber Optic Sensors*, F. T. S. Yu and S. Yin eds. Marcel Dekker, New York, Basel, 2002.
3. N. E. Fisher, D. J. Webb, C. N. Pannell, D. A. Jackson, L. R. Gavrilov, J. W. Hand, L. Zhang, and I. Bennion, "Ultrasonic Hydrophone Based on Short In-Fiber Bragg Gratings ," Appl. Opt. **37,** 8120–8128 (1998).
4. A. D. Kersey, M. A. Davis, H. J. Patrick, M. LeBlanc, K. P. Koo, C. G. Askins, M. A. Putnam, and E. J. Friebele, "Fiber grating sensors," J. Lightwave Technol. **15,** 1442–1463 (1997).
5. P. Ferraro and P. De Natale, "On the possible use of optical fiber Bragg gratings as strain sensors for geodynamical monitoring," Opt. Laser Eng. **37,** 115–130 (2002).
6. J. H. Chow, I. C. M. Littler, G. de Vine, D. E. McClelland, and M. B. Gray, "Phase-sensitive interrogation of fiber Bragg grating resonators for sensing applications," J. Lightwave Technol. **23**, 1881–1886 (2005).
7. J. H. Chow, D. E. McClelland, M. B. Gray, and I. C. M. Littler, "Demonstration of a passive subpicostrain fiber strain sensor," Opt. Lett. **30**, 1923–1925 (2005).
8. M. LeBlanc, A. D. Kersey, and T. E. Tsai, "Sub-nanostrain strain measurements using a π-phase shifted grating," in *Optical Fiber Sensors*, vol. 16 OSA Technical Digest Series (Optical Society of America, 1997), 28–30.
9. M. LeBlanc, S. T. Vohra, T. E. Tsai, and E. J. Friebele, "Transverse load sensing by use of pi-phase-shifted fiber Bragg gratings," Opt. Lett. **24**, 1091–1093 (1999).
10. A. M. Gillooly, H. Dobb, L. Zhang, and I. Bennion, "Distributed load sensor by use of a chirped Moiré fiber Bragg grating," Appl. Opt. **43,** 6454–6457 (2004).
11. S. C. Tjin, L. Mohanty, and N. Q. Ngo, "Pressure sensing with embedded chirped fiber grating," Opt. Commun. **216,** 115–118 (2003).
12. X. W. Shu, K. Chisholm, I. Felmeri, K. Sugden, A. Gillooly, L. Zhang, and I. Bennion, "Highly sensitive transverse load sensing with reversible sampled fiber Bragg gratings," Appl. Phys. Lett. **83,** 3003–3005 (2003).
13. R. W. P. Drever, J. L. Hall, F. V. Kowalsky, J. Hough, G. M. Ford, A. J. Munley, and H. Ward, "Laser phase and frequency stabilization using an optical resonator," Appl. Phys. B **31,** 97–105 (1983).

#89671 - $15.00 USD Received 12 Nov 2007; revised 3 Jan 2008; accepted 5 Jan 2008; published 28 Jan 2008

14. A. Asseh, H. Storoy, B. E. Sahlgren, S. Sandgren, and R. A. H. Stubbe, "A writing technique for long fibre Bragg gratings with complex reflectivity profiles," J. Lightwave Technol. **15**, 1419–1423 (1997).
15. S. Longhi, D. Janner, G. Galzerano, G. Della Valle, D. Gatti, and P. Laporta, "Optical buffering in phase-shifted fiber gratings" Electron. Lett. **41,** 1075–1076 (2005).
16. D. S. Elliott, Rajarshi Roy, and S. J. Smith "Extracavity laser band-shape and bandwidth modification," Phys. Rev. A **26,** 12–26 (1982).

1. Introduction

Fiber-based optic sensors are known to show several advantages as compared with conventional electro-mechanical sensors, such as electrical passive operation, electromagnetic interference immunity, multiplexing capabilities, and distributed sensing. In particular, fiber Bragg gratings (FBG's) and other grating-based devices appear to be very suited for high-sensitivity measurements of temperature, load, strain, pressure, and vibration [1, 2]. FBG strain sensors with ultra-high sensitivity are specifically required in ultrasonic hydrophones for medical sensing [3], in civil and aerospace industries for structure monitoring [4], and in geophysical surveys for measurements of seismic activity [5]. Although high-resolution FBG strain sensors are commonly based on Fabry-Perot configuration (see, for instance, [6, 7]), different and more complex FBG structures, including π-phase shifted gratings [8, 9], Moiré gratings [10], chirped gratings [11], and sampled structures [12], are more suited in certain applications, such as in transverse load sensing where extremely sharp resonances enable high-accuracy measurement of grating birefringence [9].

In this paper, we report on an optical fiber sensor with high resolution of dynamic strain. The sensor consists of a π-phase-shifted FBG interrogated by a frequency modulated laser radiation emitted from an extended cavity diode laser (ECDL), using the Pound-Drever-Hall (PDH) technique [13]. This technique is widely accepted as the best method of laser frequency stabilization and enables laser frequency noise characterizations with high accuracy. In our case, when the laser frequency is locked to the center of the FBG resonance, a broadband strain sensitivity of 5×10^{-12} Hz$^{-1/2}$ (corresponding to 5 p$\varepsilon/\sqrt{\text{Hz}}$, ε being the unit of strain) is obtained for Fourier frequencies larger than 100 kHz. This sensitivity represents a ~ 100 factor improvement compared with that demonstrated in Ref.[8], where a π-phase shifted grating was proposed for the first time as strain sensor. Moreover, it compares with the sensitivity reported in [6] using a fiber Fabry-Perot interferometer based on a uniform Bragg grating pair and the PDH technique .

2. π-shifted FBG sensor setup

The π-phase-shifted FBG used in our experiment was fabricated by the continuous writing technique [14, 15], where the UV radiation from a frequency-doubled amplitude-modulated Ar-ion laser is focused onto the core of a hydrogenated Ge-doped silica fiber (fibercore SM-28). Figure 1 shows the transmission spectrum of the 3-cm long FBG measured with a wavelength resolution of 0.2 pm. Note the appearance of the sharp resonance peak around the center of the FBG stop band at 1542.77 nm, which turns out to be splitted into two peaks spaced by 7.6 pm (corresponding to ~ 0.96 GHz) and with resolution-limited full widths at half maximum (FWHM) of 0.4 pm. Such a splitting is attributed to a weak birefringence of the fiber induced by the UV writing radiation.

The experimental setup for the implementation of the PDH method and the laser frequency stabilization is depicted in Fig. 2. An ECDL continuously tunable in the wavelength range from 1525 to 1555 nm (Toptica, model DL-100) with a maximum power of 10 mW (at a pump current of 60 mA) is used to probe the FBG reflection. The ECDL shows an emission linewidth of $\sim$ 2 MHz for observation times of few microseconds (as measured by means of the beat note with a

#89671 - $15.00 USD Received 12 Nov 2007; revised 3 Jan 2008; accepted 5 Jan 2008; published 28 Jan 2008

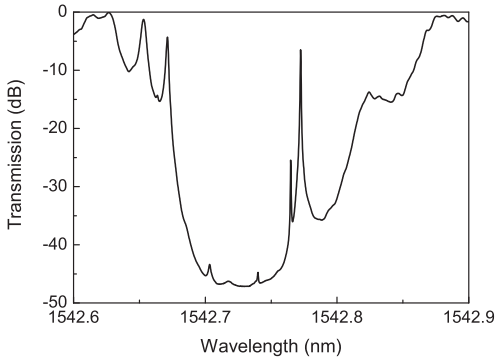

Fig. 1. Measured transmission spectrum of the 3-cm long π-phase-shifted FBG.

similar laser diode). The laser beam is coupled through an optical isolator and a $10\times$ objective to a single mode fiber. To further decrease optical feedback into the ECDL a fiber optical isolator is also used. A small amount of the laser radiation ($\sim 100\ \mu$W) is then sent to the FBG using a power splitter and an optical circulator. Grating reflection is therefore available at the optical circulator output and is monitored using a fast photodiode. One end of the π-phase shifted fiber grating is glued to a piezoelectric actuator, PZT_G, whereas the other one is fixed to a translation stage that pre-strains the fiber sensor with a total length of 1.02 m. In this way, direct calibration of the sensor strain sensitivity is performed by fiber length modulation applying a sinusoidal voltage to the PZT_G actuator. Fine frequency tuning of the laser emission around the center of the FBG stop band is obtained by supplying a linear voltage scan to the ECDL piezoelectric actuator (PZT_L). By rotating a half-wave plate placed in front of the $10\times$ launching objective a proper selection between the two FBG resonances can be performed. Figure 3(a) shows the FBG reflection signal recorded at the output of the photodiode transimpedance amplifier versus the detuning between the laser frequency and the FBG resonance. The narrowest resonance shows a linewidth of 55 MHz and a minimum reflection of 26%.

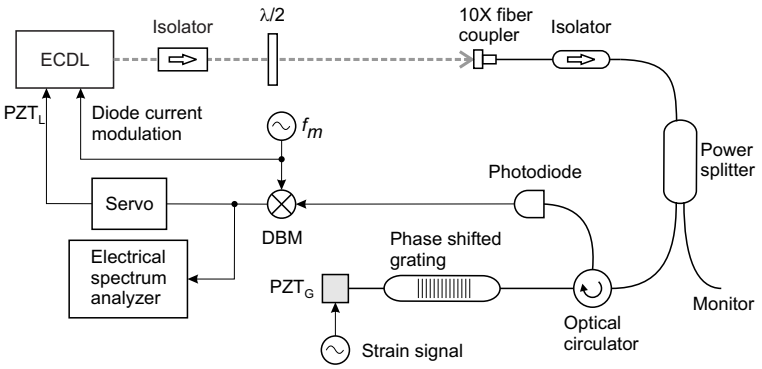

Fig. 2. PDH experimental setup using an ECDL and a π-phase-shifted FBG. PZT: piezoelectric transducer; $\lambda/2$: half-wave plate for input polarization control; DBM: doubled-balanced mixer.

#89671 - $15.00 USD Received 12 Nov 2007; revised 3 Jan 2008; accepted 5 Jan 2008; published 28 Jan 2008

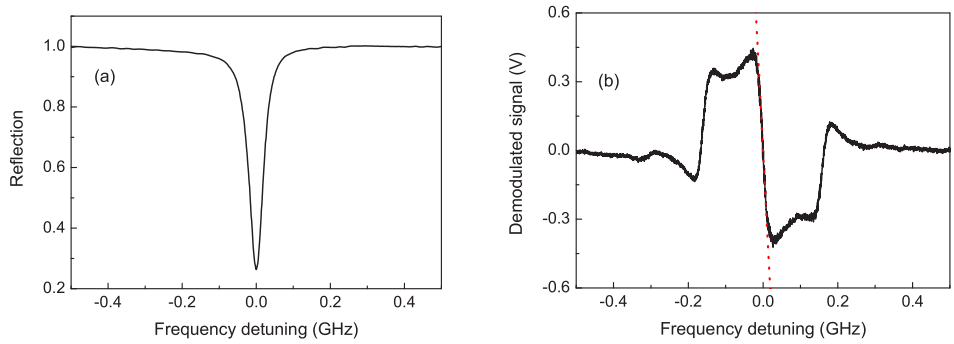

Fig. 3. (a) Measured FBG reflection signal at the output of the transimpedance amplifier versus frequency detuning (10 kHz measurement bandwidth). (b) Demodulated reflection signal at the output of DBM versus frequency detuning (10 MHz measurement bandwidth). In (b), the dotted curve represents the linear interpolation of the recorded trace around the resonance center frequency, corresponding to a discriminator slope of 32 nV/Hz.

3. FBG sensor characterization

To implement the PDH technique the laser field is frequency modulated by means of a sinusoidal modulation of the pump diode current. A modulation frequency $f_m = 202.7$ MHz, about four times larger than the FBG resonance linewidth, and a frequency deviation equal to f_m (corresponding to an unitary phase-modulation index) were used in order to provide high signal to noise ratio [13]. The reflected signal from the FBG was preferred rather than transmitted one, due to its higher sensitivity [13]. Figure 3(b) shows the in-phase demodulated lineshape of the FBG reflection, with a measurement bandwidth of 10 MHz, at the output of the doubled balanced mixer as a function of the frequency detuning. This signal is an odd function of the frequency detuning (discriminating signal) and therefore can be used as an error signal to measure the fluctuations between the laser frequency and the FBG resonance, and to lock the laser to the FBG resonance center. From the recorded data a voltage to frequency conversion coefficient of 32 nV/Hz, corresponding to the slope of the demodulated signal at the resonance center (see dotted line in Fig. 3(b)), was obtained. To lock the laser frequency against the FBG resonance, the demodulated signal was fed back to the high-voltage piezoelectric amplifier through an integral and proportional servo electronics. A typical control loop bandwidth of ~ 1 kHz was used. This control bandwidth was fast enough to efficiently suppress the long-term laser frequency drifts and the environmental noise, and enabled a tight laser frequency locking even when the optical system was subject to strong environmental perturbations.

The dynamic strain applied to the FBG sensor can be measured by monitoring the error signal directly at the output of the doubled-balanced mixer for Fourier frequencies larger than the control loop bandwidth. Indeed, according to the model proposed by Kersey *et. al.* [4], the relative deviation of the Bragg wavelength (frequency) is related to the applied strain, ε, by the following expression:

$$\frac{\Delta\lambda_B}{\lambda_B} = \frac{\Delta\nu_B}{\nu_B} = K\varepsilon, \tag{1}$$

where λ_B (ν_B) is the fiber Bragg resonance wavelength (frequency), $\Delta\lambda_B$ ($\Delta\nu_B$) is the Bragg wavelength (frequency) deviation induced by the applied strain, and $K \simeq 0.78$ is a constant related to the Poisson's ratio and Pockels coefficients of the photoelastic tensor of the fiber

#89671 - $15.00 USD Received 12 Nov 2007; revised 3 Jan 2008; accepted 5 Jan 2008; published 28 Jan 2008

glass [4]. The power spectral density of the applied strain is therefore given by:

$$S_\varepsilon(f) = \frac{S_{\Delta\nu}(f)}{(\nu_B K)^2} = \frac{S_V(f)}{(\nu_B K D)^2} \quad [\varepsilon^2/\mathrm{Hz}] \tag{2}$$

where $S_V(f)$ is the power spectral density of the error signal, D is the voltage to frequency conversion coefficient, and $S_{\Delta\nu}(f) = S_V(f)/D^2$ is the power spectral density of the frequency fluctuations between the laser and the FBG resonance frequencies.

Figure 4 reports the measured noise spectral density of the error signal, when the laser locking is operating, as recorded directly at the intermediate frequency output of the doubled balanced mixer (IF bandwidth: from DC to 10 MHz). For Fourier frequencies larger than the $\sim$ 1-kHz control loop bandwidth, the spectral noise density is well described by the polynomial $S_V(f) = 7\times10^{-6} f^{-1} + 6\times10^{-10}$ V^2/Hz, which sets the lower limit to the sensor strain sensitivity, and by few peaks located at 1.08, 1.65, 6, and 14.8 kHz due to laser piezo resonances and mechanical vibrations. For Fourier frequencies lower than 1-kHz the spectral noise density is strongly reduced by the optoelectronic servo locking and is characterized by several peaks due to line components (50 Hz and its harmonics) and acoustic noise (21 Hz, 42 Hz, and 710 Hz). Using the experimental data for the voltage to frequency conversion coefficient at the mixer output $D = 32$ nV/Hz, a Bragg frequency $\nu_B = 194$ THz, and $K = 0.78$ the power spectral density $S_\varepsilon(f) = 3\times10^{-19} f^{-1} + 2.6\times10^{-23}$ ε^2/Hz is calculated from Eq. (2). For frequencies larger than 100 kHz, a white power strain spectral density of 2.6×10^{-23} ε^2/Hz is obtained, corresponding to a strain sensitivity of 5 p$\varepsilon/\sqrt{\mathrm{Hz}}$. This limit is ascribed to the ECDL white frequency noise, which turns out to be $S_{\Delta\nu}(f) = 5.9\times10^5$ Hz^2/Hz. Such frequency noise corresponds to an emission linewidth $\Delta\nu_l = \pi S_{\Delta\nu} \simeq 1.9$ MHz [16], in good agreement with the 2-MHz value retrieved by the beat note measurement. Calibration of the sensor strain sensitivity was performed applying a sinusoidal voltage signal with an amplitude of 50 mV to the

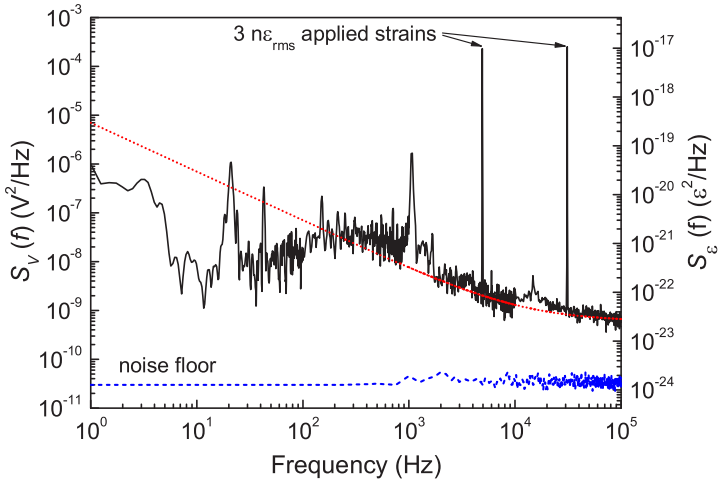

Fig. 4. Measured power spectral density of the voltage signal at the output of the doubled-balanced mixer. The right vertical axis shows the converted power spectral density of the strain, $S_\varepsilon(f)$, using eq.(2) and assuming $D = 32$ nV/Hz, $K = 0.78$, and $\nu_B = 194$ THz. Red dotted line is the best polynomial noise interpolation of the power spectral density for $f \geq 1$ kHz; blue dashed line represents the electronic noise floor.

#89671 - $15.00 USD Received 12 Nov 2007; revised 3 Jan 2008; accepted 5 Jan 2008; published 28 Jan 2008

fiber grating piezoelectric actuator, which produced in the noise spectrum shown in Fig. 4 two marked peaks at the modulation frequencies of 5 and 30 kHz. Assuming a PZT actuating coefficient of 89 nm/V and taking into account the 1.02 m length of the fiber sensor, the applied strains correspond, in both cases, to a root mean square value of 3 nε. This calibration leads to strain sensitivities over 1-Hz bandwidth of 10 pε and 6 pε at frequencies of 5 and 30 kHz, respectively, in excellent agreement with the strain spectral noise density deduced by Eq. (2).

As far as the dynamic range of the FBG sensor is concerned, the maximum strain that can be observed is limited to frequency change of the FBG resonance lower than its linewidth. Considering the 55-MHz FBG linewidth, the maximum detectable strain is ~ 350 nε, corresponding to a dynamic range of 97 dB (over 1-Hz bandwidth) for Fourier frequencies above 100 kHz. It may be noted that strains larger than 350 nε can be detected for frequencies lower than 1-kHz control loop bandwidth, using either the error signal at the IF output of the doubled balanced mixer or the control signal at the output of the high-voltage piezoelectric amplifier. In this case, however, the sensitivity is lower, due to the $1/f$ flicker noise contribution.

4. Conclusion

A fiber-based strain sensor showing a power spectral density of $S_\varepsilon(f) = (3\times10^{-19}f^{-1} + 2.6\times 10^{-23})$ Hz^{-1} for a wide Fourier frequency interval from 1 kHz to 10 MHz and a dynamic range of 97 dB (in 1 Hz measurement bandwidth) was demonstrated using a π-phase shifted fiber Bragg grating interrogated by a phase-modulated laser radiation in a Pound-Drever-Hall configuration. The 5×10^{-12} Hz$^{-1/2}$ best sensitivity of the passive fiber Bragg grating sensor turns out to be limited solely by the frequency noise contribution of the probing laser source. The proposed fiber sensor has potential applications in the field of ultra-high-resolution ultrasonic hydrophone for medical sensing and sonar systems.

#89671 - $15.00 USD Received 12 Nov 2007; revised 3 Jan 2008; accepted 5 Jan 2008; published 28 Jan 2008